Seasonal and vertical variation in canopy structure and leaf spectral properties determine the canopy reflectance of a rice field

Weiwei Liu, Matti Mõttus, Jean-Philippe Gastellu-Etchegorry, Hongliang Fang, Jon Atherton

Agricultural and Forest Meteorology 355 (2024) 110132

Contents lists available at ScienceDirect

Agricultural and Forest Meteorology

journal homepage: www.elsevier.com/locate/agrformet

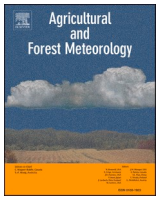

Seasonal and vertical variation in canopy structure and leaf spectral properties determine the canopy reflectance of a rice field

Weiwei Liu [a,e,*], Matti Mõttus [b], Jean-Philippe Gastellu-Etchegorry [c], Hongliang Fang [d], Jon Atherton [e]

[a] College of Resources and Environment, Fujian Agriculture and Forestry University, Fuzhou, 350002, China
[b] VTT Technical Research Centre of Finland, PO Box 1000, 02044, VTT, Finland
[c] Toulouse III University, Center for the Study of the Biosphere from Space (CESBIO), CNRS, CNES, IRD, Toulouse University, 18 Avenue Edouard Belin, 31401, Toulouse, France
[d] LREIS, Institute of Geographic Sciences and Natural Resources Research, Chinese Academy of Sciences, Beijing, 100101, China
[e] Optics of Photosynthesis Laboratory, Institute for Atmospheric and Earth System Research (INAR)/Forest Sciences, University of Helsinki, PO Box 27, 00014, Helsinki, Finland

ARTICLE INFO

Keywords:
Radiative transfer simulation
Canopy structure
Leaf inclination angle
Clumping
Seasonal and vertical variation

ABSTRACT

Physical model simulations have been widely utilized to simulate the reflectance of vegetation canopies. Such simulations can be used to estimate key biochemical and physical vegetation parameters, such as leaf chlorophyll content (LCC), leaf area index (LAI), and leaf inclination angle (LIA) from remotely sensed data via model inversion. In simulations, field crops are typically regarded as one-dimensional (1D) vegetation canopies with constant leaf properties in the vertical direction and across the growing season. We investigated the seasonal effects of these two simplifications, 1D canopy structure, and vertically constant leaf properties, on canopy reflectance simulations in a rice field using *in situ* measurements and the 3D discrete anisotropic radiative transfer model (DART). We also developed a new methodology for reconstructing 3D crop canopy architecture, which was validated using measurements of gap fraction and canopy reflectance. Our results revealed that the 1D canopy assumption only holds during the early stage of the growing season, then leaf clumping affects canopy reflectance from the jointing stage onwards. Consideration of the 3D canopy structure and its seasonal variation significantly reduced the deviation between simulated and measured canopy reflectance in the green and near-infrared wavelengths when compared to the typical 1D canopy assumption and produced the closest multi-angular distribution pattern to the measurements. The vertical heterogeneity of leaf spectra affected canopy reflectance weakly during the maturation stage when senescence started from the bottom of the canopy. Consideration of seasonal and vertical variation in LIAs significantly improved the results of 1D canopy reflectance simulations, including the multi-angular distribution patterns. In contrast, the directionally-averaged clumping index (CI) only slightly improved the 1D canopy reflectance simulation. To summarize, these findings can be used to reduce the simulation bias of canopy reflectance and improve the retrieval accuracy of key vegetation parameters in crop canopies at the seasonal scale.

1. Introduction

Physically-based canopy radiative transfer (RT) models have been widely used to simulate canopy reflectance and retrieve key canopy structure parameters (Houborg et al., 2007, 2015; Kimm et al., 2020) and, when coupled to leaf reflectance models, leaf traits such as leaf chlorophyll content (LCC) (Zarco-Tejada et al., 2004; Croft et al., 2015, 2020a). Physically-based model simulations are the baseline for understanding the impact of vegetation parameters on remote sensing measurements, being able to account for different observation configurations, canopy structures and ground optical properties and due to their sound theoretical basis (Verrelst et al., 2010). Further, physically-based models are critical to the success of satellite retrievals of the aforementioned structural parameters and leaf traits. Such retrievals have been developed using a diverse variety of computational methods including lookup tables (Zarco-Tejada et al., 2004; Croft et al.,

* Corresponding author.
E-mail address: weiweiliu@fafu.edu.cn (W. Liu).

https://doi.org/10.1016/j.agrformet.2024.110132
Received 1 November 2023; Received in revised form 6 April 2024; Accepted 19 June 2024
Available online 27 June 2024

2015; Houborg et al., 2015), machine learning (Bacour et al., 2006) and hybrid models (Xu et al., 2019a), and model simulation results, including reflectance and vegetation indexes, are usually the input parameters or training data of such retrieval methods. Hence model simulation accuracy greatly influences retrieval accuracy (Gara et al., 2019; Li et al., 2020a).

Physically-based models are generally classified into two types according to the structural characteristics of specific vegetation (Croft et al., 2020a). Three-dimensional (3D) canopy RT schemes were developed to model spatially heterogeneous canopies, such as forests and shrubs (Chen and Leblanc, 1997). Simpler one-dimensional (1D) canopy RT models were used for 'homogeneous' canopies, such as agricultural crops and grass (Verhoef, 1984). Hence the first and foremost simplification in crop canopy reflectance modelling is describing crop canopies as simplified 1D homogeneous media. The 1D simplification vastly simplifies the modelling burden, unlike in the more complex 3D schemes. This simplification is therefore widely applied for example in the estimation of LCC and LAI of field crops, with the SAIL model serving as an exemplar (Verhoef, 1984; Jacquemoud et al., 2009; Berger et al., 2018; Croft et al., 2020b; Xu et al., 2019a, 2022). However, for a heterogeneous vegetation canopy, use of 1D canopy RT models is questionable due to the underestimation of radiation penetration and the inaccurate simulation of canopy reflectance (Duthoit et al., 2008; Govind et al., 2013), which then impact the parameter retrievals in the inversion process (Fang et al., 2019; Croft et al., 2020a).

Nonetheless, clumping is present in crop canopies (Duthoit et al., 2008; Ma et al., 2022) and is known to vary across the growing season as crops grow and subsequently senesce modulating their structures; such changes can be quantified by the clumping index (CI) (Mõttus, 2004). CI was developed to characterize the non-random (i.e., 3D) distribution of foliage components in space (Nilson, 1971; Chen et al., 2005) and directly regulates the within-canopy light environment and canopy radiation transfer (Chen et al., 2021; Li et al., 2023a). Although the clumping phenomenon of crop canopies and its seasonal variation is quantifiable by *in situ* measurements (Fang et al., 2019) and satellite inversions (Wei et al., 2019; Fig. 9), the effects of the 1D canopy simplification on crop canopy reflectance simulations are still not fully understood. In addition to CI, another plant structural parameter, leaf inclination angle (LIA), deserves careful consideration when modelling radiative transfer processes (Ryu et al., 2010; Pisek et al., 2013; Zou and Mõttus, 2015; Fang et al., 2021; Yang et al., 2023). The importance of LIA is well known but it is hard to measure and therefore generally regarded as a species-specific constant for crops during the whole growing season. As with clumping, the LIA varies over the season, across functional types and through the depth of the canopy (Hagemeier et al., 2019; Pisek et al., 2020; Yang et al., 2023). Potentially, CI and LIA could be incorporated into 1D schemes to improve crop reflectance simulations, but the efficacy of such an improvement over the whole growing season is still an open question due to the lack of measurement data, including leaf, canopy spectra, and detailed 3D crop structure data.

The second simplification in crop canopy reflectance modelling is that canopy structure parameters and leaf spectral properties are generally regarded as constant across the canopy vertical profile throughout the whole growing season. However, vertical gradients of canopy structure properties have already been identified and investigated (Li et al., 2015; Fang et al., 2019; 2021) across various plant functional types. In addition, spatial-temporal variation in structural parameters regulates the 3D light environment within the canopy (Ellsworth et al., 1993; Béland and Baldocchi, 2021), which shapes the vertical gradients of leaf spectral properties (Ciganda et al., 2008; Niinemets et al., 2015; Atherton et al., 2017). For this reason, the seasonal influence of constant vegetation properties in the vertical direction on canopy reflectance simulations remains unclear and further investigation is needed. Although several studies on the impact of vertical variation in leaf properties on canopy reflectance are available, they rely on statistical techniques (Ciganda et al., 2012) or 1D RT models extended and layered in vertical dimension (Wang et al., 2013; Yang et al., 2017).

The objective of this study is to investigate the seasonal impacts of two widely used simplifications—the assumption of a homogeneous canopy and the assumption of constant vegetation properties in the vertical direction—on crop canopy reflectance simulations. To this end, a detailed investigation was performed using a 3D RT model and extensive *in situ* measurements of sufficient quality and rigour at the seasonal scale. The 3D Discrete Anisotropic Radiative Transfer (DART) model was adopted as it can simulate canopy reflectance with either 1D or 3D simulation scenes, and with either constant or variable vegetation properties in the vertical direction (Gastellu-Etchegorry et al., 1996, 2017). This enabled the investigation of the mixed effects of 1D canopy simplifications and the vertical heterogeneity of leaf traits and optical properties on crop canopy reflectance. This investigation aims not only to improve the simulations of crop canopy reflectance and the retrievals of key vegetation parameters, but also the simulations of photosynthesis and heat fluxes at the global scale (Braghiere et al., 2020; 2021; Li et al., 2024).

To achieve our goal, we collected canopy structural and spectral measurements (*cf.* Sections 3.1 and 3.2) in a paddy rice field, a crop of prime agricultural importance in Asia and beyond (Fang et al., 2014), and developed a series of 3D rice architecture models throughout the growing season (*cf.* Section 3.3.1). These 3D architecture models were used to parameterize the 3D Discrete Anisotropic Radiative Transfer (DART) model. The corresponding 1D rice scenes were generated by the DART model for the canopy reflectance simulations using the homogeneous canopy assumption. Both 1D and 3D simulations were parameterized with homogeneous and heterogeneous vertical profiles of vegetation properties, respectively. The mixed impact of the two simplifications on simulated canopy reflectance was quantified and compared with nadir and multi-angular reflectance measurements across the growing season (*cf.* Section 3.3.2). Finally, we studied the extent to which the reflectance simulations can be improved in 1D canopy models by the inclusion and modification of two canopy structure parameters, CI and LIA (*cf.* Section 3.3.3).

2. Materials and methods

2.1. Field measurements

2.1.1. Measurement site

The measurements were carried out at the Baisha Experimental Station of Fujian Agriculture and Forestry University (FAFU) in Fuzhou City, Fujian Province, China (26.237°N, 119.060°E). The site belongs to a subtropical monsoon climate with an average annual rainfall of 1706 mm and an average annual temperature of 18.5°. Measurements were carried out in a 50×30 m rectangular rice field (variety Zhongzheyou No.8) which was planted according to the standard agronomic practice with a row distance of about 30 cm and spacing in rows of about 25 cm. Eleven sets of measurements were made from June to October, covering the growing season in 7–10 day intervals, to track the major growing stages of rice (Fang et al., 2014). Table 1 shows the measurement time and the main rice canopy characteristics of each measurement, including growing stage, height, LAI, FVC, vertical layering and canopy floor. The canopies were classified into one to three horizontal layers according to the leaf number and leaf vertical location on the stem at different growing stages (Fig. 2). More specifically, a one-layer canopy was adopted during the tillering stage (measurement Nos.1–2) because the leaf vertical locations on stem were similar for all leaves, while a two-layer (measurement Nos.3–5) and three-layer canopy (measurement Nos.6–11) was adopted because the leaf vertical locations on stem are distributed at two and three vertical heights, respectively.

2.1.2. Canopy structure measurements

Digital hemispherical photography (DHP) images were taken using a Nikon D7500 camera with a 4.5 mm F2.8 EX DC circular fisheye

Table 1
Rice canopy characteristics at different measurement times. LAI: leaf area index, FVC: fractional vegetation cover, DOY: day of year.

Measurement number	Date (DOY)	Growing stage	Height (m)	LAI (m^2/m^2)	FVC	Number of layers	Canopy floor
No.1	24th July (205)	Transplanting	0.37	0.54	0.11	1	Water
No.2	31st July (212)	Tillering	0.57	1.23	0.32	1	Water
No.3	6th August (218)	Tillering	0.73	2.14	0.58	2	Water
No.4	13th August (225)	Tillering	0.89	2.98	0.70	2	Water
No.5	20th August (232)	Jointing	0.93	4.15	0.63	2	Water
No.6	30th August (242)	Jointing	1.09	4.85	0.68	3	Water
No.7	11th September (254)	Jointing	1.31	5.39	0.68	3	Water
No.8	20th September (263)	Flowing	1.40	5.97	0.88	3	Water
No.9	29th September (272)	Maturation	1.39	5.7	0.82	3	Water
No.10	9th October (282)	Maturation	1.37	3.73	0.80	3	Water
No.11	20th October (293)	Maturation	1.37	3.18	0.71	3	Soil

converter. At least eight (average of twenty) downward-looking photos were taken per measurement at 0.4–1.2 m height above the canopy to characterize an elementary sampling unit (Weiss et al., 2004). DHP images were then processed using the CAN EYE software (version 6.4.91) to extract canopy structural variables, including LAI, CI, canopy-averaged LIA and multi-angular gap fraction with an angular resolution of 2.5° for both zenith and azimuth angles. The measured LAI was used for the parameterization of the 1D homogeneous vegetation scenes (Section 2.3.1). The measured CI and canopy-averaged LIA was used for the improved 1D simulations (Section 2.3.3). The measured multi-angular gap fractions were used for the evaluation of model-based gap fraction simulations (Section 2.3.2).

Leaf inclination angles (LIA) were measured using a protractor equipped with a plumb line. Five rice clusters were selected and marked as close as possible but outside of the observation region of the spectrometer. Ten randomly selected leaves were measured in each layer (Table 1) for each marked rice cluster, i.e., 50 LIA measurements per layer. All measurements were carried out at sunset under calm conditions to avoid the effect of heat and wind on leaf angles. The measured LIA profiles were used for the reconstructions of 3D rice scenes (Section 2.3.1) and for the improved 1D simulations (Section 2.3.3).

2.1.3. Leaf chlorophyll content (LCC) measurements

Three to five rice plants were picked up randomly from the field outside the spectrometer's observation region and then transported to the laboratory using a freezer with temperature between 5 and 10 °C. The plants were cut into one to three segments according to the number of layers at the specific measurement time (Table 1). We cut a part of a leaf weighting 0.2 g from each segment and determined its area from a photograph. Leaf total chlorophyll *a* and *b* content (in units of mg/g) were measured using the anthrone reagent method with UV-VIS spectroscopy (Lichtenthaler and Buschmann, 2001) and, finally, LCC in $\mu g/cm^2$ were obtained using the photographically determined area of the leaf part. It should be noted that LCC was not used for the canopy reflectance simulations because the measured leaf reflectance and transmittance spectra were used directly in the DART model. The LCC measurements were carried out to demonstrate the vertical heterogeneity in leaf pigments (Section 3.2) and to explain the vertical variations of leaf reflectance.

2.1.4. Optical measurements

Leaf optical measurements were made using a FluoWat leaf clip (Alonso et al., 2007) connected to an HR2000 spectrometer (Ocean Optics, USA) using the measurement procedure described in Van Wittenberghe et al. (2015). The spectrometer has a spectral sampling resolution of 0.5 nm and a spectral range of 400 to 850 nm. Three to five rice leaves were collected from each layer of the field and immediately measured to avoid loss of leaf moisture.

Canopy optical measurements were carried out on a 3.5 m ladder using the same spectrometer used for leaf optical measurement with most measurements taken around 11:00 a.m. when there was no visible clouds. An optical fibre was fixed to a 1.5 m measurement pole at a constant height of 2.0 m above the rice canopy across the growing season, keeping the diameter of measurement footprints at the top of the rice canopy (shown as the red circles in Fig. 1) constant at approximately 0.9 m, a value greatly exceeding row spacing, for nadir viewing. This measurement setup was adopted to reduce the impact from different field of views of sensor for row crops (Zhao et al., 2015). The nadir reflectance measurements were repeated ten times by rotating the measurement pole to cover a larger area. Besides nadir viewing, the fibre input was tilted ±45° and ±60° (shown as red stars in Fig. 1) along the row direction for multi-angular measurement. All measurements were collected under clear sky conditions, and white panels were measured both at the beginning and end of the canopy reflectance measurements. The shadow of the operator and ladder were kept out of the measured area. The reflectance spectra of the surface below the canopy (i.e., water or soil) were also measured after the canopy reflectance measurement.

2.1.5. 3D structural measurements

Three categories of 3D structural measurements were collected *in situ* from five randomly selected rice plants using a ruler and protractor: (1) stem diameter and length; (2) location of each leaf, leaf height, leaf length, and leaf azimuth angle; (3) leaf inclination angle for each leaf. One rice plant was selected, and its leaves were divided into ten segments of equal length to measure the leaf shape functions (Zou et al., 2014). The 3D structural information was used to characterise and reconstruct a 3D rice plant based on a statistical method, modified and improved from Chang et al. (2019) using the Matlab code *3D-Crops-Model* (see Data and Code Availability of Statement for link and description).

2.3. Model parameterization and simulation

2.3.1. DART model and parameterization

We used the DART model in DART-Lux mode (Wang et al., 2022) to simulate the radiative budget and Bi-directional Reflectance Factor (BRF) of the rice canopy. Individual 3D rice plants were reconstructed with the statistical structural information as mentioned in Section 2.1.5. A series of 3D rice plants were generated randomly using the measured norm and standard deviation of each structural variable. 3D rice scenes were then constructed using the Matlab code *3D-Crops-Scene* (Data and Code Availability of Statement) using the measured row distance and rice cluster spacing in rows (30 cm and 25, respectively). The number of individual rice plants in a cluster was approximately 15 and the LAI of the 3D rice canopy matched the DHP-measured value ('True LAI').

Next, we generated a series of 1D homogeneous vegetation scenes with small triangular leaves randomly distributed within the canopy space with a spherical normal distribution and a LAI matching the measured value from the DHP images (Section 2.1.2) to simulate a turbid medium. We used triangles small enough (0.008 cm^2) to mimic the behaviour of a turbid medium classically used to simulate vegetation in models such as SAIL (Malenovský et al., 2021). Measured leaf optical

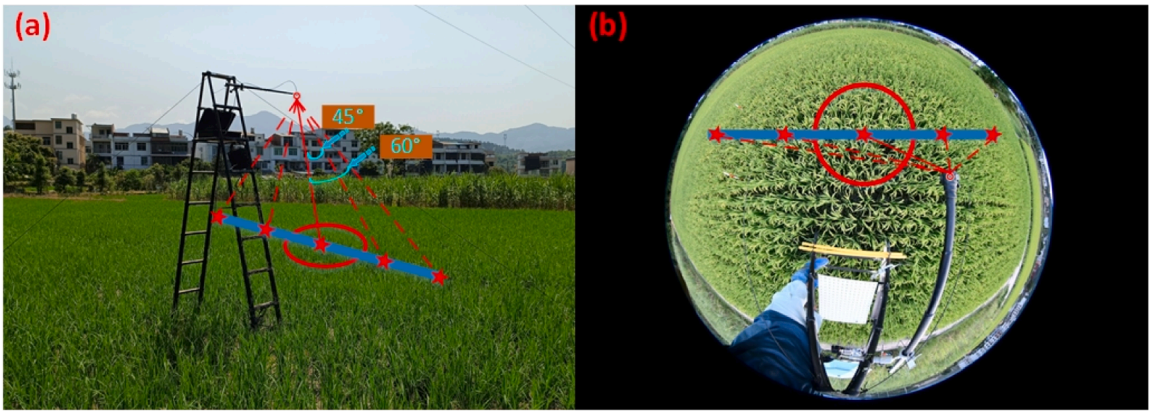

Fig. 1. Measurement set-up for collecting nadir and multi-angular canopy reflectance. (a) Side view; (b) down-ward view by a fisheye camera. Red solid and dashed lines refer to the viewing directions of nadir and multi-angular measurements. The red circle is the footprint of the bare optical fibre, the blue line indicates the tilting direction during multi-angular measurement, and the red stars are the centre points of footprints.

measurement data (i.e., reflectance and transmittance) were used for both 1D and 3D rice scenes. Each model type was parameterized to have either two or three layers with variable optical properties or the same leaf properties of the upper leaf for the whole canopy.

The solar and view geometry was the same as the measured values. The row direction of 3D rice scenes was from *in situ* measurements to account for the row structure effect (Zhao et al., 2010). The United States standard atmosphere model (NOAA, NASA, and Air-Force, U.S., 1976) with the rural area aerosol model and a visibility of 23 km was used for the canopy reflectance simulation.

2.3.2. Gap fraction simulations

The gap fraction ($P(\theta)$) is the faction of soil (or water and other backgrounds) seen in a given direction (Baret et al., 1995). Canopy gap fractions were calculated as a ratio of the intercepted radiance by ground to the total radiance intercepted by leaf and ground (Eq. (1)):

$$P(\theta) = \frac{RB_{ground}^{intercepted}(\lambda)}{RB_{leaf}^{intercepted}(\lambda) + RB_{ground}^{intercepted}(\lambda)} \quad (1)$$

where $RB_{leaf}^{intercepted}(\lambda)$ and $RB_{ground}^{intercepted}(\lambda)$ are the intercepted radiance of all plant components and the ground-intercepted radiance at the wavelength λ, respectively. We used the DART model in DART-FT mode to simulate radiative budget. The "Intercepted" term is the 1D and 3D vegetation radiative budget at the end of the direct sun illumination stage (i.e., "Illudir" stage) before the scattering stage (Liu et al., 2020).

For the 3D rice scenes, gap fractions were simulated with zenith angles varying from 0° to 60° in a 5° interval in three azimuth angles: (1) parallel to the row direction; (2) vertically to the row direction; and (3) at 45° to the row direction. For the 1D rice scenes, gap fractions were simulated with the same zenith angles but with only one azimuth angle.

2.3.3. Canopy reflectance simulations

Canopy reflectance simulations were carried out for two purposes: (I) comparisons of 1D and 3D simulations with two vertical profiles of leaf optical properties (Section 3.3.2); and (II) evaluation of three improved methods for 1D simulations (Section 3.3.3). For I, four types of simulations were used (Table 2): (1) 3D Rice + homo_profile: 3D rice scene with the homogeneous vertical distribution of leaf spectra, (2) 3D Rice + hete_profile: 3D rice scene with the heterogeneous vertical distribution of leaf spectra, (3) 1D Rice + homo_profile: 1D rice scene with the homogeneous vertical distribution of leaf spectra and (4) 1D Rice + hete_profile: 1D rice scene with the heterogeneous vertical distribution of leaf spectra. For II, three improved simulation methods for a 1D canopy, CI-scaled, LIA-adjusted-profile and LIA-adjusted-average, were proposed and tested in this study. For the CI-scaled method, CI determined from directionally averaged DHP images was used to scale the 'real' LAI (LAI_{real}) to obtain an effective LAI (LAI_{effect}) used in the simulations (Eq. (2)). For the LIA-adjusted methods, actual measured LIA profile and canopy-averaged LIA were used in the simulations of LIA-adjusted-profile and LIA-adjusted-average, respectively. As a reference, we used 1D rice with heterogeneous leaf optical properties and a spherical distribution of leaf angles.

$$LAI_{effect} = LAI_{real} \times CI \quad (2)$$

3. Results

3.1. Seasonal and vertical variations of canopy structure

The seasonal variations in LAI and its division between the canopy layers are shown in Fig. 2a. The total canopy LAI measured by DHP increased with the development of canopy leaves and reached a maximum of 5.50 at the 8th measurement (No. 8), after which it

Table 2
Four types of canopy reflectance simulations (purpose I) and three improved methods for 1D simulations (purpose II).

Simulations types	Simulation scenes	Vertical leaf spectra	LAD	Canopy clumping
3D Rice + homo_profile	Reconstructed 3D Rice scene	Homogeneous (only upper layer)	Measured LIA (upper, middle, and bottom layers)	Yes
3D Rice + hete_profile	Reconstructed 3D Rice scene	Heterogeneous (upper, middle, and bottom layers)	Measured LIA (upper, middle, and bottom layers)	Yes
1D Rice + homo_profile	1D turbid scene	Homogeneous (only upper layer)	Spherical LAD	NO
1D Rice + hete_profile	1D turbid scene	Heterogeneous (upper, middle, and bottom layers)	Spherical LAD LIA-adjusted-profile LIA-adjusted-average (Section 3.3.3)	NO CI-scaled (Section 3.3.3)

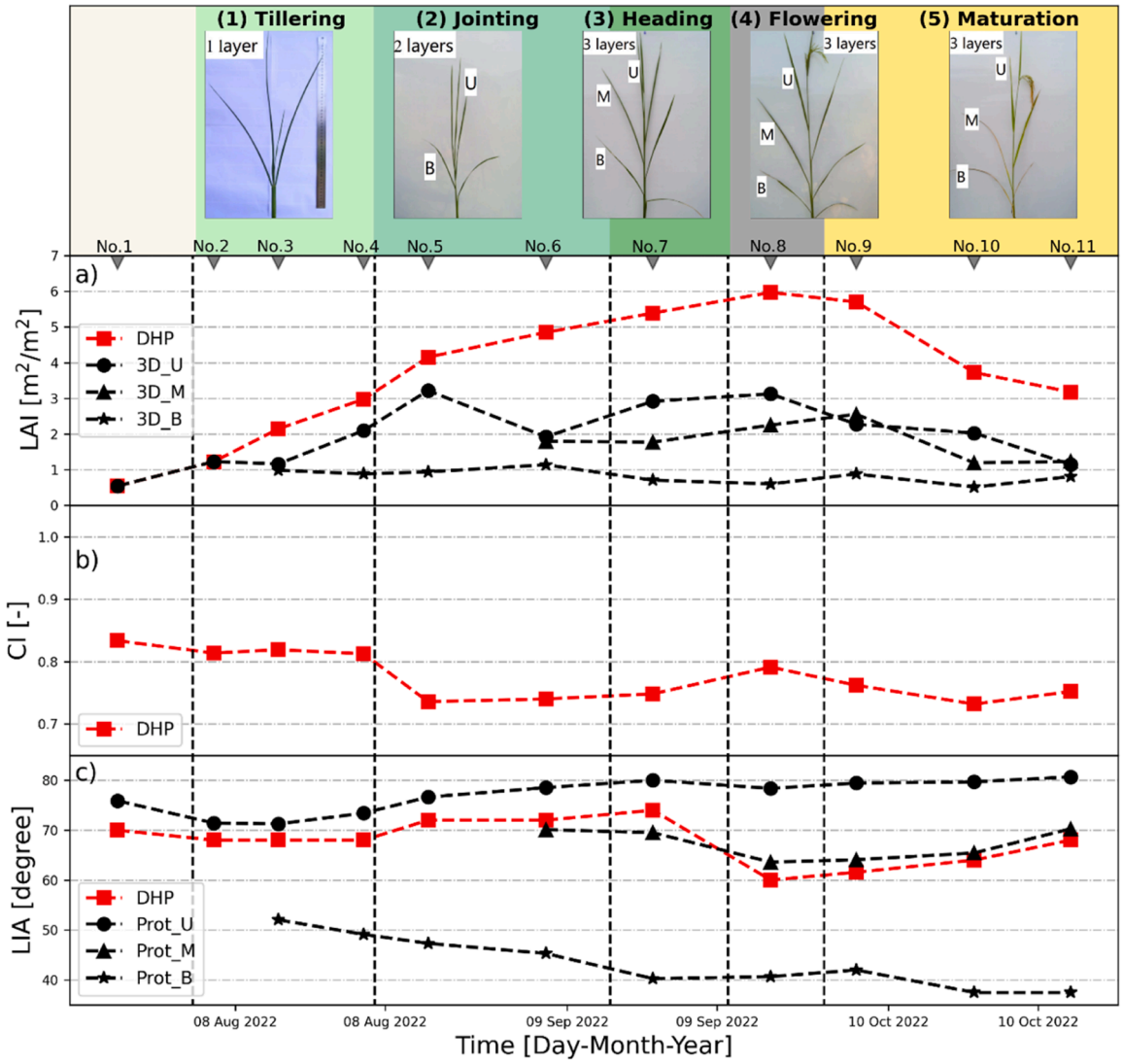

Fig. 2. Seasonal and vertical variation of LAI (a), CI (b), and LIA (c): upper layer (circle, 'U'), middle layer (triangle, 'M'), lower layer (bottom, 'B'), and whole canopy (square). The canopy-level LAI, CI, and LIA were measured by DHP. The LAI (a) and LIA (c) profiles were retrieved from the reconstructed 3D rice scenes. Measurement No.1 represents the transplanting stage.

gradually decreased as the leaves senesced. The statistically-based measurement (3D reconstructed rice) shows the seasonal variation of LAI at three layers. During the heading, flowering, and maturation stages a three-layer canopy formed, and LAI decreased gradually in the upper layer and was almost constant in the middle and bottom layers. CI values varied from 0.83 to 0.73 across the season (Fig. 2b): starting above 0.80 at the transplanting and tillering stages, CI quickly decreased to 0.73 once rice entered the jointing stage. It remained stable until harvest, with a small temporary increase to 0.79 at the flowering stage (measurement No.8). A negative relationship (not shown) was found between LAI and CI during the growth process of rice, meaning that the variation of CI is related to the number of leaves.

The mean canopy LIA measured by DHP remained almost constant at 70° for the tillering stage and then increased gradually to 75° from the jointing to the heading stages (Fig. 2c). Interestingly, canopy mean LIA decreased rapidly from 75° to 60° in ten days from the heading to the flowering stages and then gradually increased again to about 70° during the maturation stage. Fig. 2c also shows the vertical LIA profile measured separately for the three layers using a protractor. LIA of the upper layer had similar variation to canopy mean LIA before the heading stage and then remained almost constant until the maturation stage. LIA of the middle layer had similar variation to canopy mean LIA from the heading to the maturation stage, including a rapid decrease between the heading and flowering stages. LIA of the bottom layer decreased gradually from the jointing to the maturation stage. The leaf inclination angle distributions (LAD) during measurements 1–4 are similar to spherical LAD (see detail in Fig. 1S), after which LIA exhibited clear spatial and temporal variation. A negative relationship was found between LIA and CI during the whole growth process of rice, even during the short-term phase (measurement No.8).

3.2. *Seasonal and vertical variations of leaf properties*

The leaf and canopy chlorophyll content (LCC and CCC, respectively) had similar seasonal variation for the three layers: they increased slightly during the tillering stage and then decreased gradually until the end of the season (Fig. 3a). LCC had a vertical gradient (upper > middle > bottom) from the heading to the maturation stages. Leaf reflectance at 550 nm increased gradually across the growing season along with the decrease in LCC in all three layers (Fig. 3b). In contrast, reflectance at 800 nm showed no remarkable seasonal variation for the upper and middle layers but decreased from the heading stage for the bottom layer (Fig. 3c). Leaf reflectance in the bottom layer was remarkably different from the upper and middle layers across the season. A more detailed

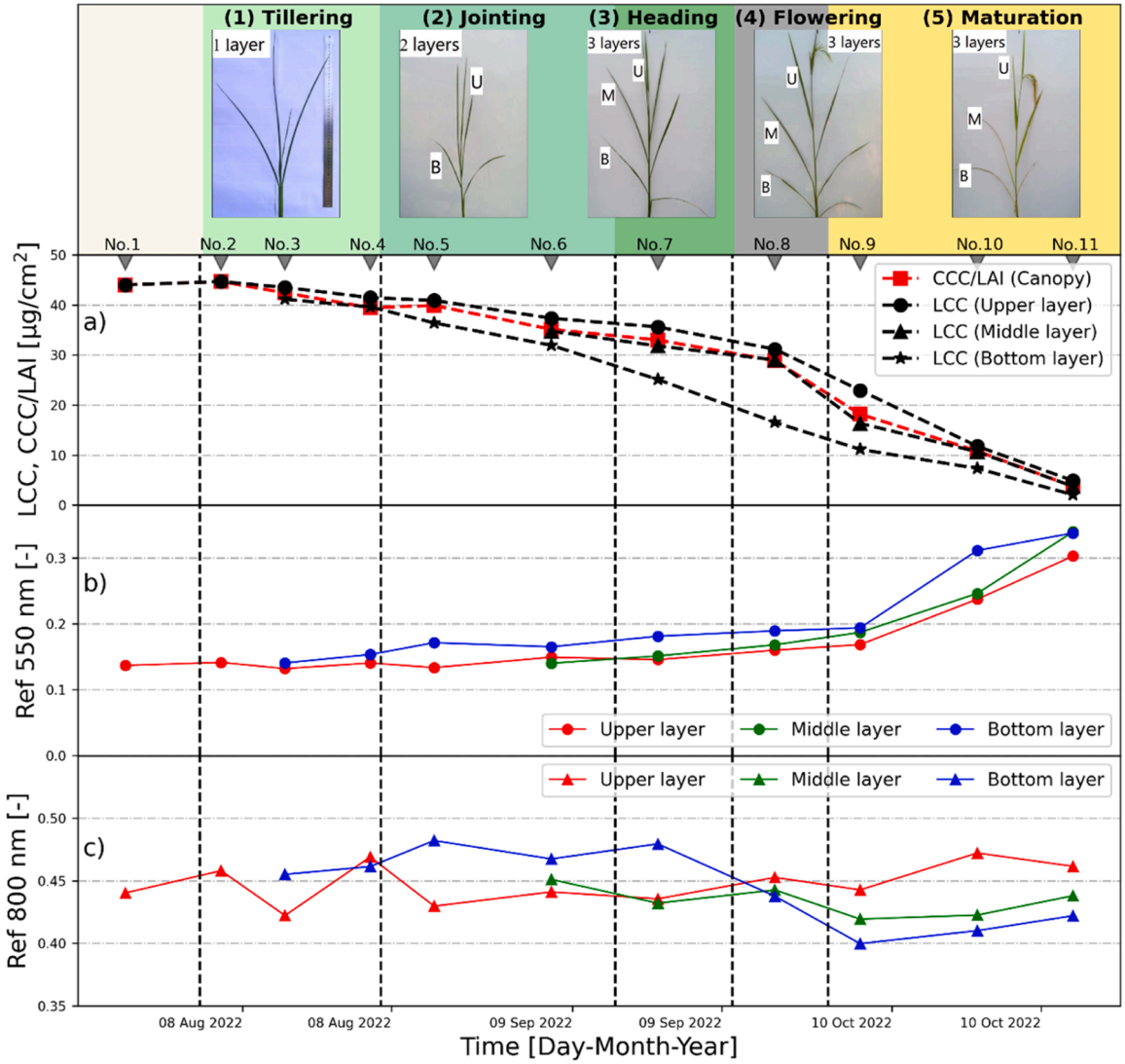

Fig. 3. Seasonal and vertical variation in chlorophyll content (LCC: leaf chlorophyll content, CCC: canopy chlorophyll content normalized by canopy LAI) and leaf reflectance at two wavelengths (550 and 800 nm). Five representative pictures of the corresponding growing stage of rice are shown above the figure. Measurement No.1 represents the transplanting stage.

presentation of the seasonal and vertical variations of leaf reflectance from 400 to 850 nm is given in Fig. 4. The spectral discrepancy amongst the layers was slightly visible from the jointing stage and was remarkable during the maturation stage.

3.3. Seasonal simulations and comparisons of canopy reflectance

3.3.1. 3D rice simulations

Fig. 5 (a-k) shows individual 3D rice plants and scenes at different growing stages reconstructed using the measured statistics. The seasonal variation in gap fraction (Fig. 6) was inversely related to LAI (Fig. 2a) with a decrease from the transplanting to the jointing stage and then an increase until the maturation stage. Similar to LIA, a period of rapid change occurred between measurements No. 7 and 8 (Fig. 6g and h). The gap fraction of 3D rice scenes matched well with the DHP values: R^2 of 0.98 and RMSE of 0.03 for the whole growing season (Fig. 6l). The correlation for 1D rice scenes was weaker: R^2 of 0.8 and RMSE of 0.09 for the whole growing season (Fig. 7l). During the tillering stage, the gap fraction of 1D scenes agreed relatively well with the measured values (Fig. 6b-d). During the jointing stage, the gap fractions of the 1D rice scenes were generally larger than those of the measured and simulated scenes (Fig. 6e-g). A systematic difference appeared in the jointing stage with larger differences in canopies with larger gap fractions. During the maturation stage, the gap fractions of 1D scenes only match well with the measured values for the small gap fraction (Fig. 6i-k). Amongst the three azimuth angles, the simulated gap fractions using 1D homogeneous scenes parallel to the row direction (circle) produced the largest errors, especially in the tillering stage (Fig. 6b).

3.3.2. 1D and 3D simulations with two vertical profiles

Fig. 7 shows the seasonal courses of rice canopy reflectance in the nadir direction of *in situ* measurements and the four types of model simulations (i.e., 1D and 3D rice scenes with homogeneous or heterogeneous layers). The model simulations using 1D rice scenes systematically overestimated canopy reflectance in the green (by up to 98%) and NIR (by up to 38%) spectral regions, especially between the jointing and maturation stages. In contrast, the canopy reflectance simulated by the 3D rice scene matched well with the measurements across the growing season in the whole spectral region (see Fig. S2 for details) and showed fewer deviations with the measurement than the 1D simulations (reduced to 0–59% for green wavelengths and 1–29% for NIR wavelengths). Vertically heterogeneous leaf spectra ('hete_profile' in Fig. 7) mainly impacted the simulation of canopy reflectance during the maturation stage (Fig. 7i and j) when the layered 3D rice scenes

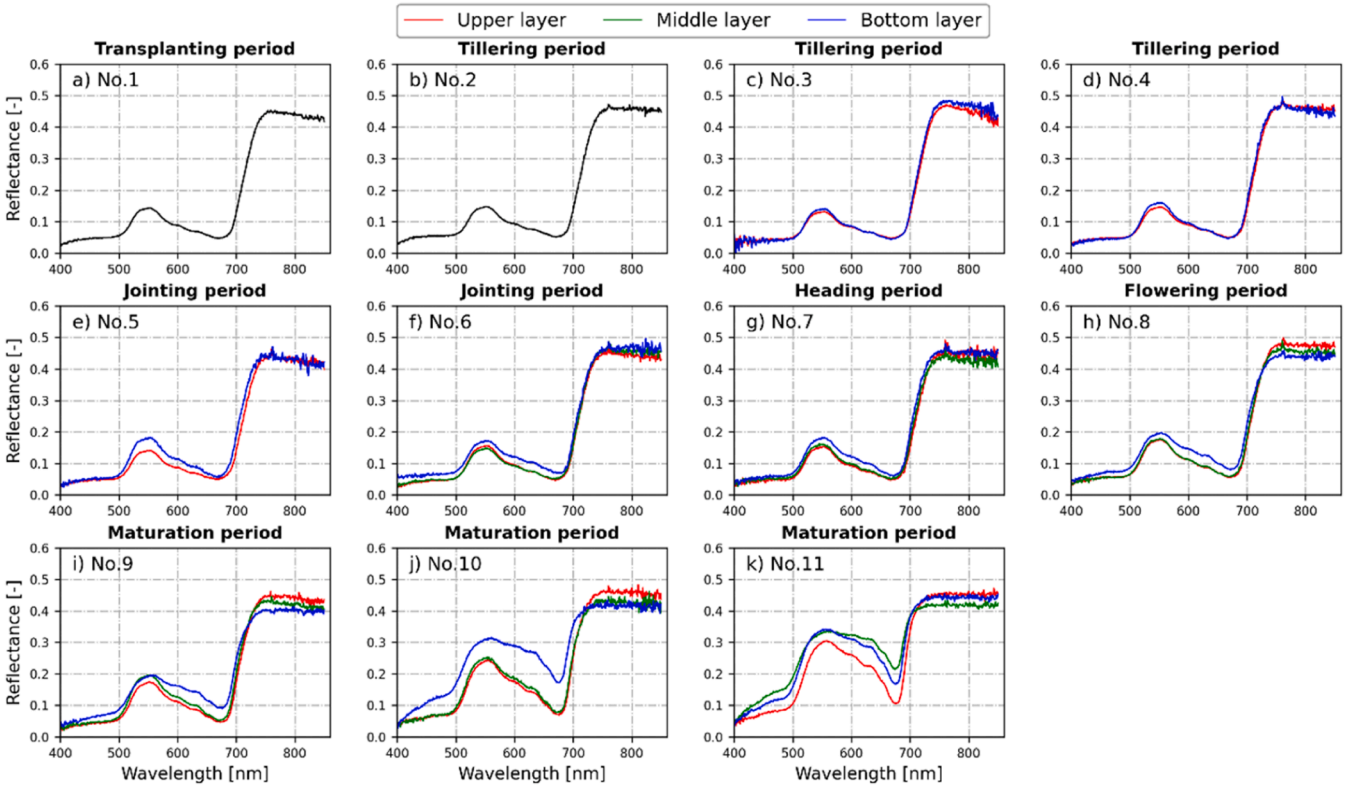

Fig. 4. Seasonal and vertical variation in leaf reflectance spectrum measured with the FluoWat clip. Red line: samples from the upper canopy layer; green line: middle layer; blue line: bottom layer.

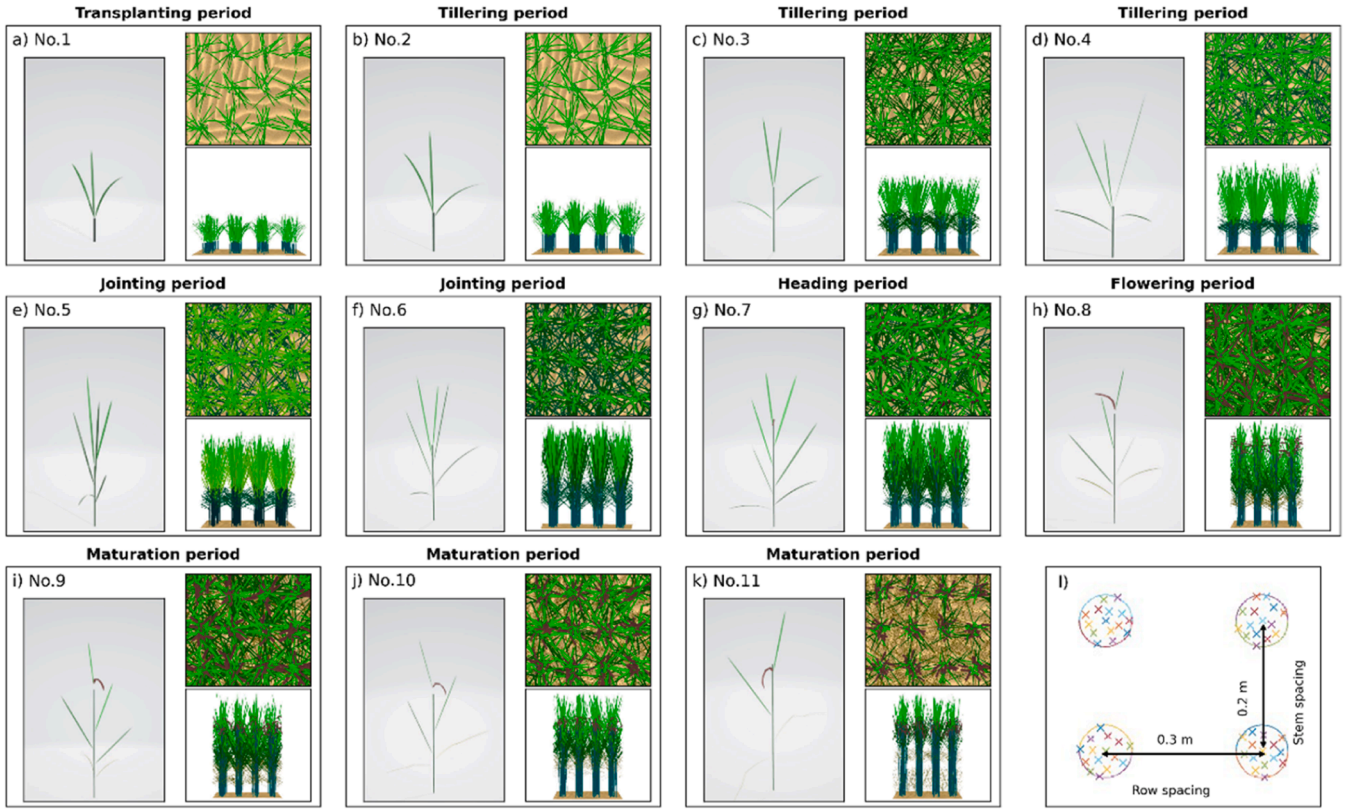

Fig. 5. Statistically-based 3D reconstruction of 3D rice plants and scenes. Each panel shows an individual rice plant, and the nadir and side views of the scene, respectively. Fig. 5l shows the locations of the rice plants.

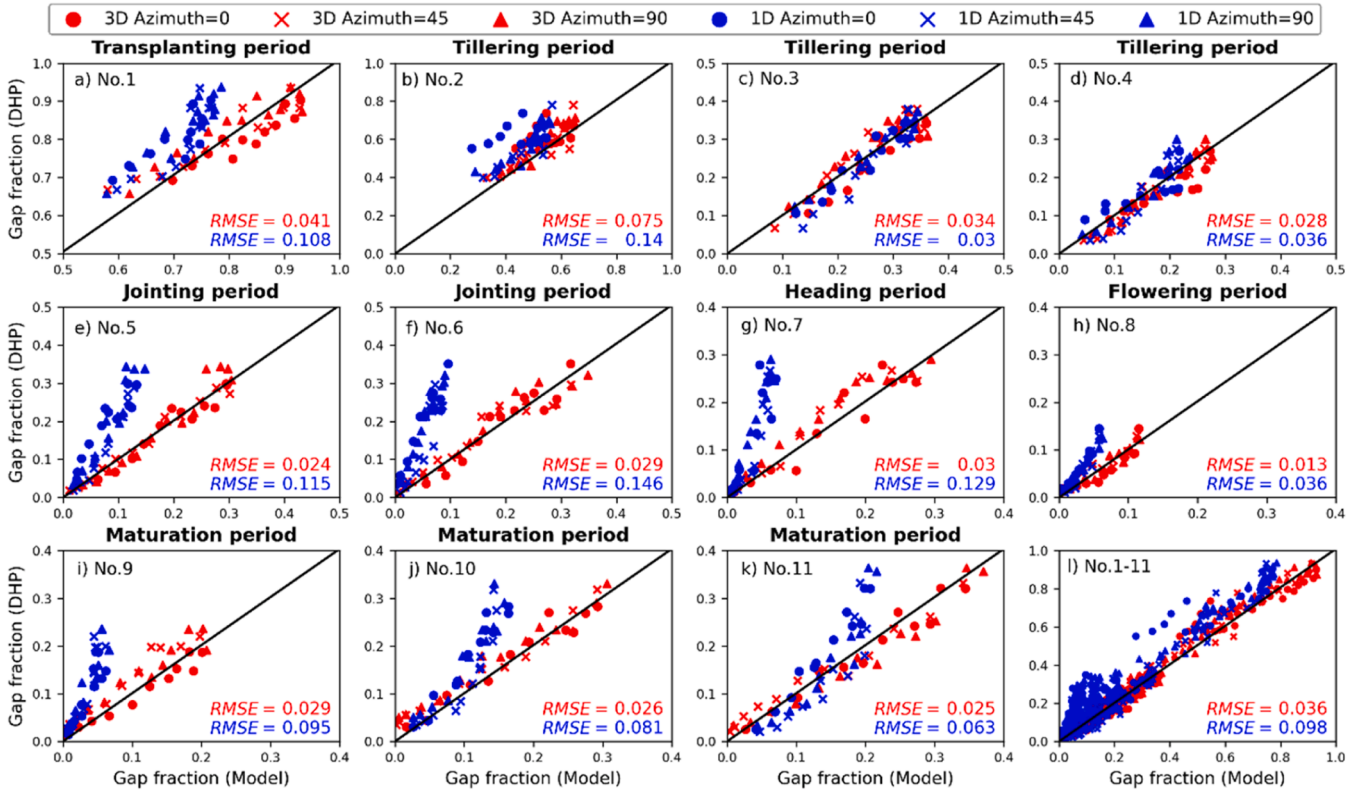

Fig. 6. Seasonal and directional comparison of measured and simulated gap fractions in 3D rice scenes (in red) and 1D homogeneous scenes (in blue). The circle and triangle denote gap fractions parallel and vertically to the row direction, respectively, and the cross marks the gap fractions at 45° to the row direction.

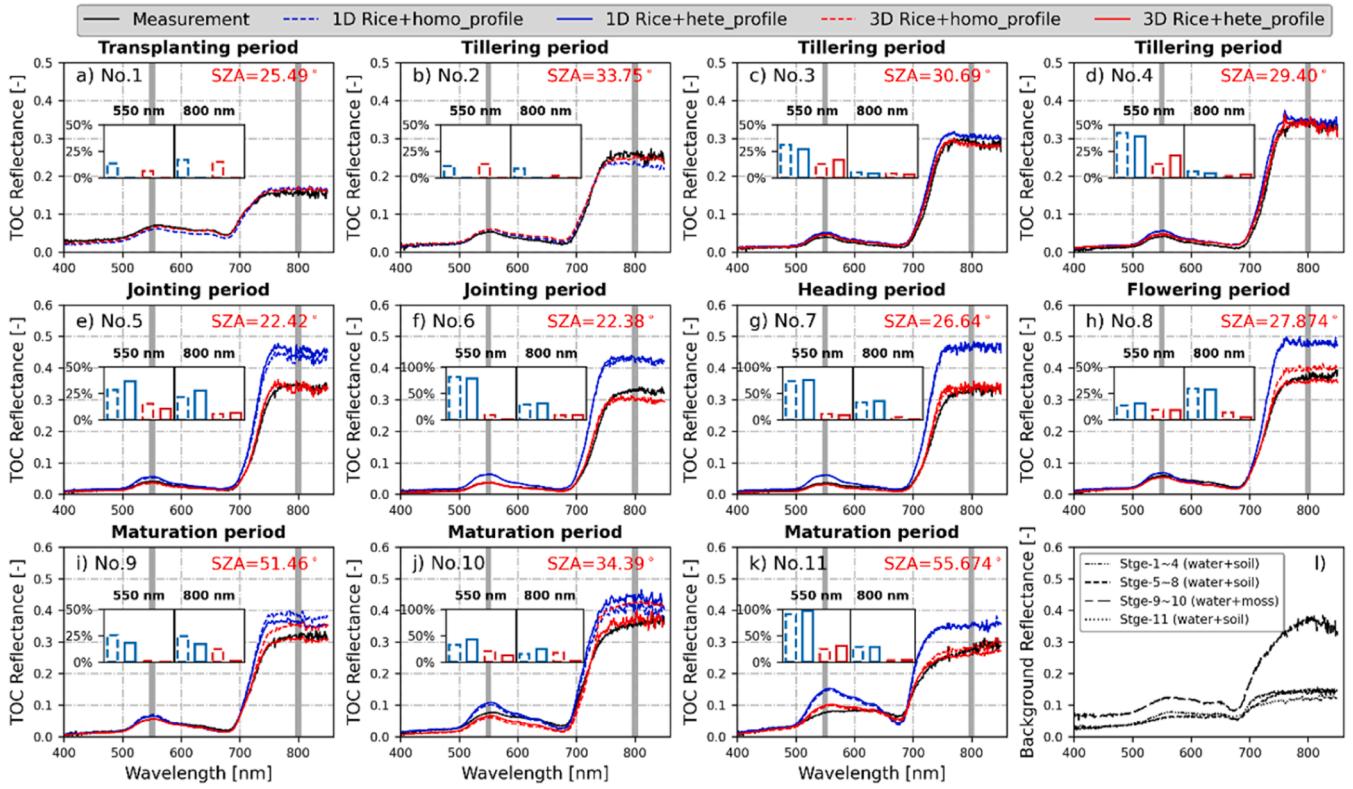

Fig. 7. Seasonal variation of the measured and simulated rice canopy reflectance from both 1D and 3D scenes. 'homo_profile' and 'hete_profile' are the scenes with the homogeneous and heterogeneous vertical distribution of leaf spectra, respectively. SZA is the instantaneous solar zenith angle. The deviation percentages at 550 and 800 nm are shown in the embedded graphs.

produced the reflectance best matching the *in situ* measurements.

Fig. 8 compares the modelled and measured multi-angular canopy reflectance (550 and 800 nm) at the four growing stages. Canopy reflectance curves simulated with both 1D and 3D scenes are bowl-shaped with somewhat different angular distributions. For instance, the angular distribution pattern at the jointing stage (Fig. 8f and j) shows the most marked bowl shape, with reflectance ratios of 2.66 (550 nm) and 1.93 (800 nm) for the backward direction (−65°/0°) and reflectance ratios of 2.78 (550 nm) and 2.00 (800 nm) for the forward direction (65°/0°). Reflectance simulations with the 3D scenes produced a similar angular distribution pattern with measurements at 550 nm (Fig. 8e-h) and 800 nm (Fig. 8i-l). In contrast, 1D canopy reflectance simulations

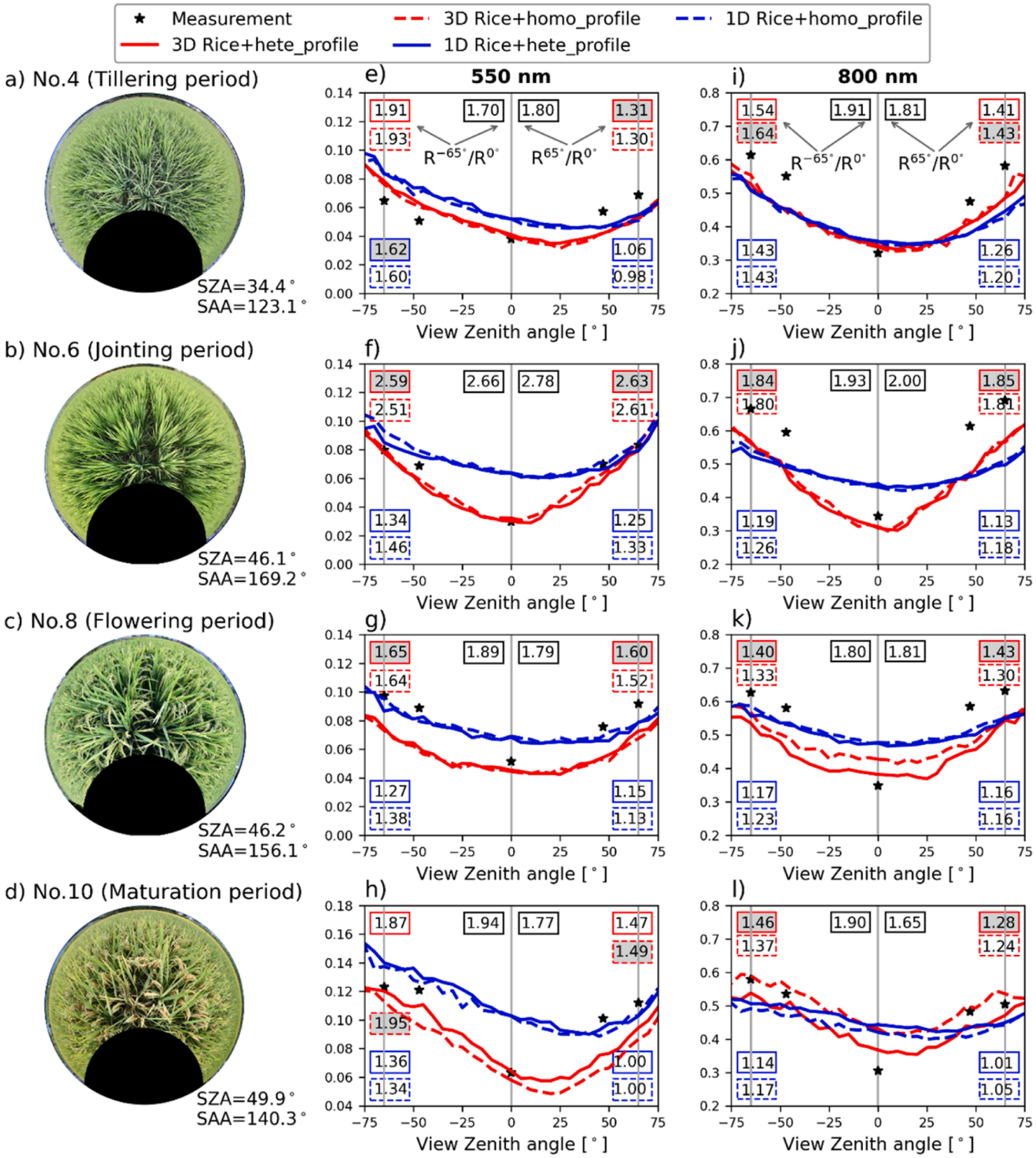

Fig. 8. DHP images of the actual rice canopy (first column) and the multi-angular variation in canopy reflectance at 550 nm (second column), and 800 nm (third column) from model simulations (coloured lines) and measurements (black star). The reflectance ratios at two view zenith angles are shown in each subgraph: −65°/0° for the backward side (left with colour) and 65°/0° for the forward side (right with colour). The best-matched reflectance ratios with measurement values are filled with grey colour.

produced less marked bowl-shaped angular distributions with overestimated reflectance at the nadir direction. Vertically heterogeneous leaf spectra ('hete_profile' in Fig. 8) had only a weak impact on the angular distribution pattern in the 3D scenes at the flowering and maturation stages.

3.3.3. 1D simulations with adjusted LAI and LIA

Use of effective LAI (the CI-scaled simulation) in the 1D simulations only slightly improved the reflectance prediction in the NIR region, from 750 nm to 850 nm, but had little effect on the overestimation in the green wavelengths, from 500 nm to 600 nm (Fig. 9). In contrast, use of *in situ* measured LIA profiles in the 1D simulations (the LIA-adjusted-profile simulation) improved results markedly in the NIR producing an even closer fit with the measurement, and removed the overestimation in the green region. Furthermore, reflectance simulations with the LIA-adjusted-profile method produced a similar angular distribution pattern with measurements at 550 nm and 800 nm (Fig. 10). Although there were mismatches between the canopy reflectance measurement and LIA-adjusted-profile 1D simulation in the green region during the maturation stage, the LIA-adjusted-profile method produced a closer fit to the measurement data when compared with the CI-scaled method. In addition, the use of canopy-averaged LIA in 1D simulations (the LIA-adjusted-average simulation) induced larger errors in canopy reflectance simulations relative to the LIA-adjusted-profile method, especially from the jointing stage (Figs. 9 and 10). Last, by using both CI and LIA profiles, the canopy reflectance simulations of 1D canopies were slightly improved compared with using only LIA profiles (Fig. S4).

4. Discussion

4.1. The impacts of seasonal and vertical variation in canopy structure on canopy reflectance

The penetration, multiple scattering, and escape of light from a crop canopy all depend on the distribution and sizes of gaps within the canopy (Duthoit et al., 2008). Hence, realistic parameterization of canopy gaps is central to accurate radiative transfer simulations and is also a key factor in land surface modelling, because it also influences the radiation fluxes that modulate carbon and energy balance (Braghiere et al., 2020; 2021).

The realism of our reconstructed 3D rice simulation scenes was demonstrated in the comparisons with the multi-angular measurements of gap fraction (Fig. 7, R^2 = 0.98 and RMSE = 0.03 for the whole growing season). In contrast to our 3D rice simulation canopies, the widely used 1D homogeneous canopy assumption for crop canopies (Xu et al., 2019b; Croft et al., 2020a; Zhang et al., 2023) yielded substantial errors in gap fractions for this rice field from the jointing to the maturation growing stages (R^2 = 0.80 and RMSE = 0.09 for the whole growing season).

Similarly to gap fraction, the simulated spectral reflectance of the 3D scenes was closer to the measurements than that of the 1D scenes: deviation was reduced to 0–59% at green wavelengths and 1–29% at NIR wavelengths in both nadir and inclined view directions (Figs. 8 and 9). These findings indicate that multi-angular gap fraction measurements are useful in the evaluation of 3D simulation scenes. Although the realism of 3D simulation scenes has been evaluated previously using measured leaf area density or photographs (Fournier et al., 1998; Chang et al., 2019), these evaluation methods relied only on the canopy

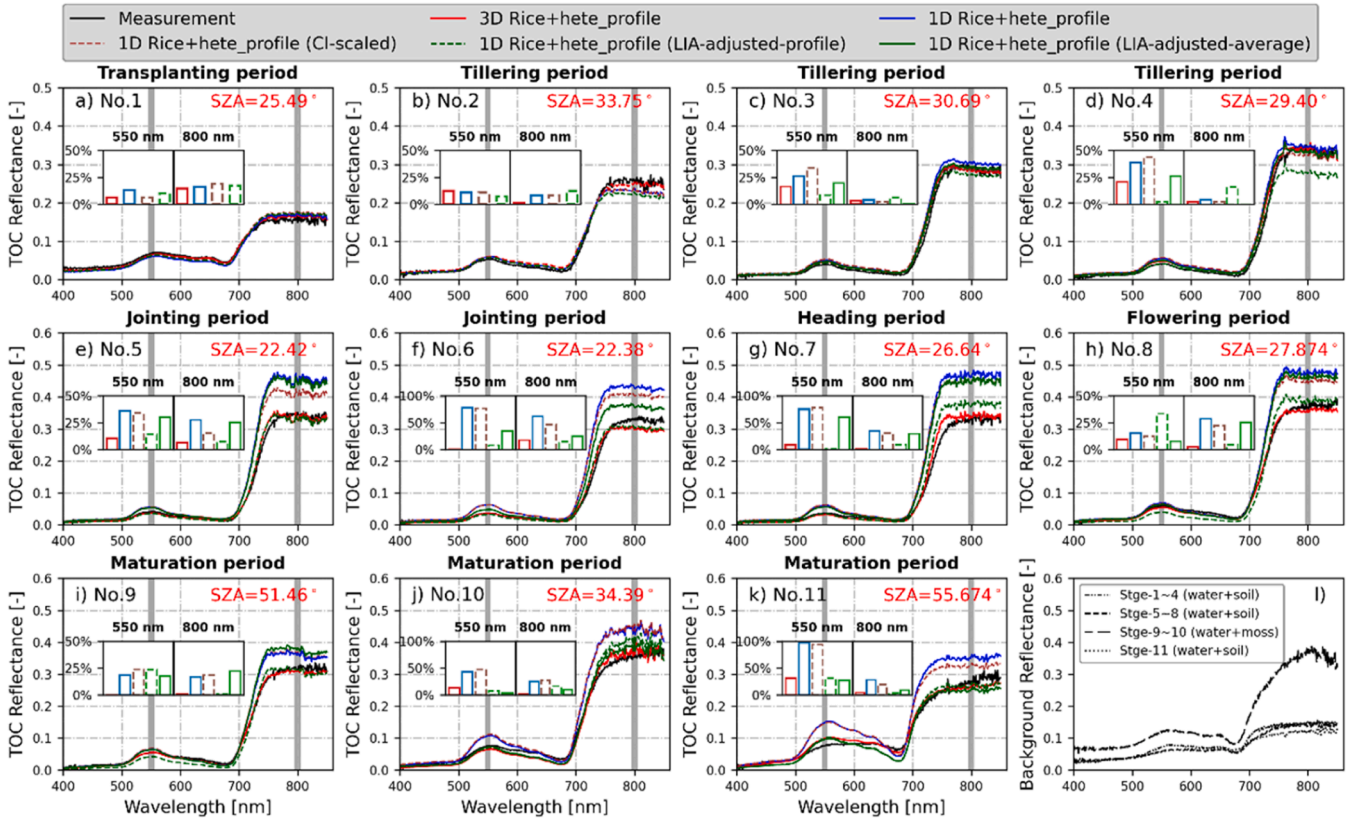

Fig. 9. Seasonal changes in reflectance of the measurement, 3D simulations, 1D simulations and three improved 1D simulation methods ('CI-scaled' 'LIA-adjusted-profile', and 'LIA-adjusted-average'). 'CI-scaled' indicated the use of effective LAI, LAI×CI. 'LIA-adjusted-profile' and 'LIA-adjusted-average' means the use of a measured LIA profile and canopy averaged LIA, respectively. SZA is the instantaneous solar zenith angle. The deviation percentages at 550 and 800 nm are shown in the embedded graphs.

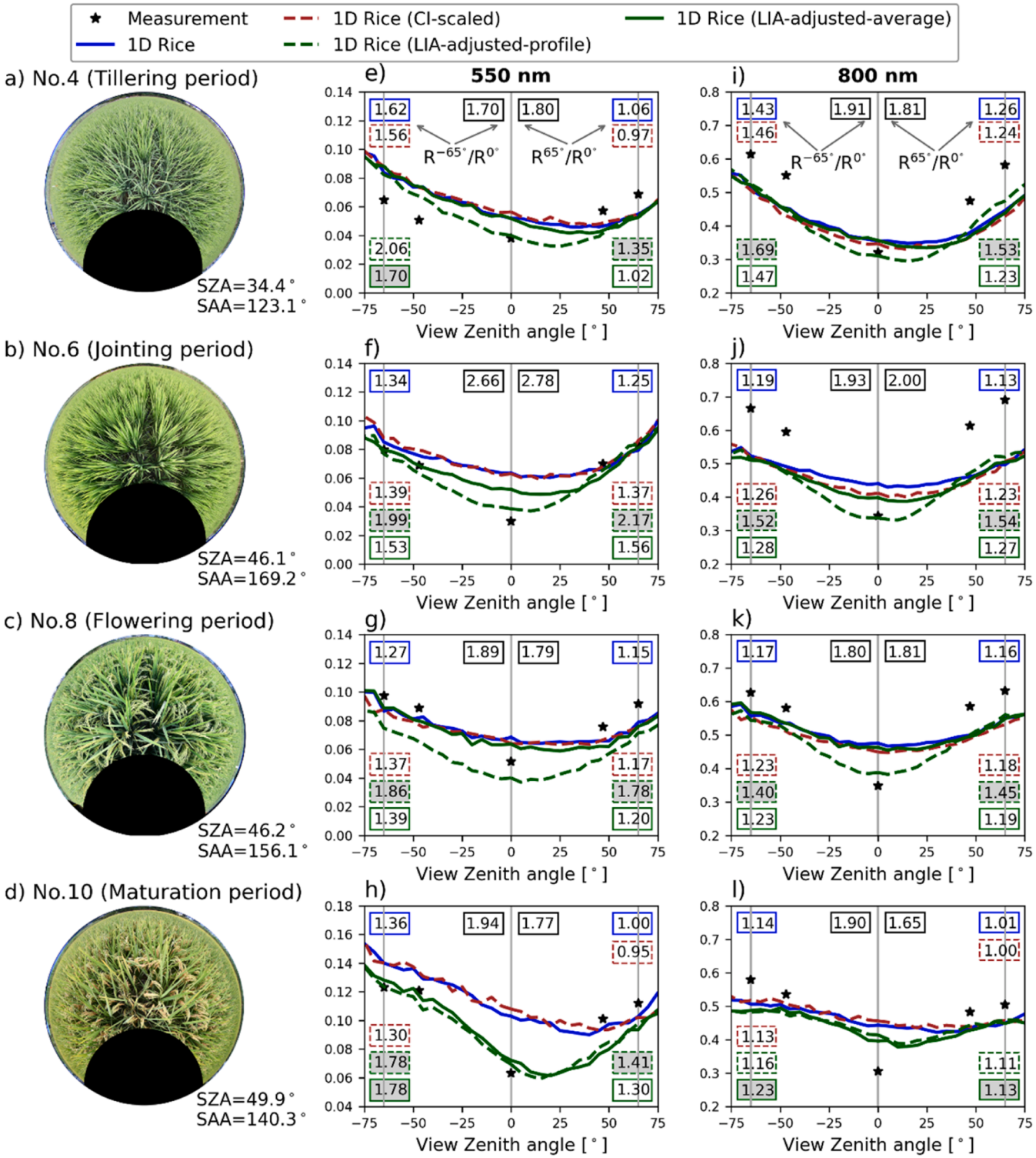

Fig. 10. DHP images of the actual rice canopy (first column) and the multi-angular variation in canopy reflectance at 550 nm (second column), and 800 nm (third column) from 1D simulations and three improved 1D simulation methods (coloured lines) and measurements (black star). The reflectance ratios at two view zenith angles are shown in each subgraph: −65°/0° for the backward side (left with colour) and 65°/0° for the forward side (right with colour). The best-matched reflectance ratios with measurement values are filled with grey colour.

structure characteristics and lacked the link between these characteristic and canopy reflectance which we show here.

The structure of the 3D rice canopy varied throughout the season (Fig. 2 and 3). Hence, the assumption that rice is a static 1D homogeneous RT medium with fixed LIA values across the season produces noteworthy deviations in canopy reflectance simulations (Fig. 7). The common assumption of crops as a homogeneous 1D medium, e.g. for the estimation of LCC (Zarco-Tejada et al., 2004; Croft et al., 2020b; Xu et al., 2019a, 2022; Xu et al., 2019b), only held at the beginning of the season, i.e., the tillering stage (Fig. 7a-d, Fig. S2ad). During this period, the 1D- and 3D-modelled gap fractions matched relatively well with the measurements (Fig. 6b-d) and no marked differences were found in the

spectral shape (Fig. 7a-d, Fig. S2a-d) nor the angular distribution (Fig. 8a) of canopy reflectance. From the jointing stage onwards, the gap fractions (Fig. 6e-h), and the spectral shapes (Fig. 7e-h, Fig. S2e-h) of 1D homogeneous and 3D rice canopy models diverged and the 1D homogeneous canopy failed to reproduce the measured angular distribution of reflectance (Fig. 8b). Hence, the use of 1D homogeneous canopy assumption affects the accuracy of retrievals of key vegetation parameters, such as LAI, CI and LCC, from multi-angular or large swath satellite data (Fang et al., 2019; 2021; Laurent et al., 2011). These findings indicate that consideration of 3D canopy structure is especially important when conducting simulations and related retrievals across the season.

As well as conducting 3D simulation, we also investigated if we could improve the 1D simulations by including additional information on canopy clumping and leaf angles gleaned from our measurements. This is important as the complexity of 3D schemes precludes their use in most current retrieval algorithms. Correction of the LAI by the directional-averaged CI in 1D canopies only slightly improved canopy reflectance simulations between 700 nm and 850 nm (Fig. 9). However, canopy clumping has angular dependencies (Fang et al., 2021) which may be relevant for rice –unlike maize (Duthoit et al. 2008).

A species-specific leaf angle distribution is widely used in crop studies (Pisek et al., 2013; Croft et al., 2020a; Xu et al., 2022). Although LIA was previously found to affect canopy reflectance mainly in the NIR region (Wang et al., 2013; Zou and Mõttus 2015), in this study, we found that using a constant spherical leaf angle distribution for all measurement dates caused substantial error in NIR reflectance (Fig. 7). We also found that correcting LIA by the measured LIA profiles in 1D canopies significantly improved the simulation of canopy reflectance (Fig. 9) and its angular distribution (Fig. 10). However, it should be noted that ignoring the vertical variation of LIA in 1D canopies reduces the efficacy of measured LIA on canopy reflectance simulations, especially from the jointing stage (Fig. 9 and 10). Importantly, without field data on leaf angles, the LIA-induced fast variation (Fig. 2c, Fig. S3) of canopy reflectance at measurement No.8 can easily be attributed to an increase in LAI because variation in LAI and LIA lead to similar changes in reflectance. To summarize, the seasonal and vertical variations in leaf inclination angles must be considered to accurately simulate crop canopy reflectance. This result underlines the difficulty of partitioning the contributions of LIA and LAI to canopy reflectance, and a potential issue with multispectral satellite LAI retrievals if leaf angle variations are not considered, due to the "ill-posed" nature of the problem (Verrelst et al., 2015).

4.2. The impacts of seasonal and vertical variation in leaf optical properties on canopy reflectance

In addition to variation in 3D canopy structure, we also investigated the importance of variation in leaf optical properties on canopy reflectance. Notable vertical variation of LCC was found starting from the heading stage. The vertical profiles of LCC also varied at the different growing stages (Fig. 3a). In general, LCC decreased inside the canopy from top to bottom, consistently with previous studies in rice (Li et al., 2020b), maize (Ciganda et al., 2008), and forest vegetation (Atherton et al., 2017; Gara et al., 2019), and in line with the light environment (Hirose et al., 1987; Lichtenthaler et al., 2007).

The variation in pigments was also visible in the measured leaf reflectance spectra (Fig. 3, 4 and Fig. S5). Differences in leaf reflectance and LCC between the layers were notable in the visible and red-edge regions from the jointing to the maturation stage (Fig. 3a-c). In the NIR region, the reflectance differences were only obvious from the flowering to the maturation stage (Fig. 6d). This could be due to the vertical variation in foliar structure or other non-pigment molecules which interact with radiation at the beginning and during the maturation stage (Di Bella et al., 2004; Zhang et al., 2005). In addition, strong relationships between LCC and leaf reflectance-based indexes were observed in each layer (Fig. S5), which provide the foundation for the LCC profile estimations using canopy reflectance.

At the canopy level, the reflectance differences caused by the vertical variations in leaf properties were noticeable in the NIR region from the flowering to the maturation stage (Fig. S2 h-k). This could be attributed to the different canopy depths sensed by the visible and NIR spectra. More specifically, the canopy reflectance spectra in the visible regions are primarily attributable to the upper leaves (Ciganda et al., 2012), while the canopy reflectance spectra in the NIR regions would better represent vertical heterogeneity due to multiple scattering and the resultant longer path lengths of canopy escaping photons. These findings are consistent with the sensitivity analysis results of Wang et al. (2013) using decreasing and homogeneous vertical profiles of biochemical parameters.

4.3. Implications and next steps

Seasonal variation of crop canopy structure is typically parameterized using LAI and CI only (Fang et al., 2019; 2021). These data are then used to constrain radiative transfer models and applied to investigate the relationships between the remotely sensed signals and leaf properties, or to retrieve leaf properties using an inversion strategy (Croft et al., 2020a). Based on our findings, we suggest a different strategy.

Scenes with 3D structure varying throughout the growing season parameterized with measured LIA profiles are clearly the best option to accurately simulate crop reflectance over the season. When there is a lack of 3D canopy structure data, variation in leaf angles and vertical profiles should still be accounted for as these can be easily confused with variations in LAI – especially if the former is assumed to be a species-specific constant. mSCOPE has accounted for the vertical heterogeneity of leaf properties and LAI (Yang et al., 2017), hence the vertical variation of LIA could be considered in future studies. This would facilitate the evaluation of the effects of the LIA profile on canopy reflectance (and also fluorescence and photosynthesis) using an improved mSCOPE model and *in situ* measurements. Although the impacts of vertical variations in leaf properties on canopy reflectance were only noticeable from the jointing to the maturation stage, this may be different for other crops with contrasting canopy structures and phenological stages, such as maize, wheat and soybean. The outline of this study, including the measurement and investigation methods, could be used as reference in future studies to clarify these issues.

The importance of LIA has been raised by many studies (Pisek et al., 2013; Yang et al., 2023). For instance, leaf inclination angles and leaf optical characteristics may change simultaneously under extreme environmental conditions (Xu et al., 2021; Hwang et al., 2023). Without measured or retrieved LIA, using canopy spectra to retrieve leaf optical characteristics is questionable. Unfortunately, LIA data (Pisek et al., 2020; Li et al., 2023a) is still rare and its retrieval methods are less studied (Zou and Mõttus. 2015). Our LIA measurement data, up to our best knowledge, is the first dataset throughout the whole growth stage of crop canopy accounting for vertical variation. However, our measurement method is time-consuming and cannot cover a larger area. Although terrestrial laser scanning (TLS) can be used to retrieve vertical LIA distribution, it is not practical for crops at the seasonal scale for frequent measurements. Furthermore, applying TLS-based methods in dense canopies (i.e., high LAI) remains challenging due to occlusion effects (Jin et al., 2021; Ali et al., 2021). Next, we plan to use levelled photography to measure LIA continuously throughout the whole growth season for main crop types, such as maize and wheat.

5. Conclusions

We investigated the impacts of seasonal and vertical variation of canopy structure and leaf spectral properties on rice canopy reflectance using 3D simulations and *in situ* measurements. The main conclusions are:

a) Rice canopies can be regarded as 1D homogeneous canopies from the transporting to the trilling stage. From the jointing stage onwards, assuming a 1D homogeneous canopy with vertically constant leaf properties leads to biased canopy reflectance simulations with systematic overestimation in the green (up to 98%) and NIR (up to 38%) spectral regions.
b) Considering the 3D canopy structure and its seasonal variation significantly reduced the error in the simulated canopy reflectance in the green (reduced to 0–59%) and NIR (reduced to 1–29%) wavelengths when compared with the 1D canopy assumption, and produced the closest angular reflectance distributions best matching the measurements.
c) Vertical variations in leaf optical property had a weak effect on canopy reflectance simulation from the flowering to the maturation stages for rice.
d) Use an angularly averaged clumping index leads to large discrepancies in NIR reflectance across the growing season and is of limited value in 1D canopy reflectance simulations of rice.
e) LIA is an important parameter in canopy reflectance models. Considering its seasonal and vertical variation improves canopy reflectance simulations even with simpler 1D models.

The findings of this study can improve the simulation of crop canopy reflectance at the seasonal scale and give an insight to the remote retrieval of key vegetation parameters. We hope that in the future, more crop types will be investigated using automatic and continuous measurements across the growing season.

CRediT authorship contribution statement

Weiwei Liu: Writing – original draft, Methodology, Investigation, Funding acquisition, Formal analysis. **Matti Mõttus:** Writing – review & editing, Methodology, Funding acquisition. **Jean-Philippe Gastellu-Etchegorry:** Writing – review & editing, Software. **Hongliang Fang:** Writing – review & editing. **Jon Atherton:** Writing – review & editing, Methodology, Funding acquisition.

Declaration of competing interest

The authors declare that they have no known competing financial interests or personal relationships that could have appeared to influence the work reported in this paper.

Data availability

The data that support the findings of this study are available on request from the corresponding author. The codes for 3D-Crops-Model (https://github.com/huananbei/3D-Crops-model) and 3D-Crops-Scene (https://github.com/huananbei/3D-Crops-Scene) are also publicly available. DART is freely available for research and education at Toulouse III University (https://dart.omp.eu).

Acknowledgments

This research has been co-financed by the Chinese Natural Science Foundation (Grant No. 42101325) and Natural Science Foundation of Fujian Province, China (Grant Nos. 2021J01210949). MM was funded by the Academy of Finland (Grant Nos. 322256 and 348035). JA was funded by the Academy of Finland (Grant No. 347929). We acknowledge Shengwei Shi and Lulu Liao (Fujian Agriculture and Forestry University) for their support of the measurements.

Supplementary materials

Supplementary material associated with this article can be found, in the online version, at doi:10.1016/j.agrformet.2024.110132.

References

Ali, B., Zhao, F., Li, Z., Zhao, Q., Gong, J., Wang, L., Tong, P., Jiang, Y., Su, W., Bao, Y., Li, J., 2021. Sensitivity Analysis of Canopy Structural and Radiative Transfer Parameters to Reconstructed Maize Structures Based on Terrestrial LiDAR Data. Remote Sens 13 (18), 3751.

Alonso, L., Gómez-Chova, L., Vila-Francés, J., Amorós-López, J., Guanter, L., Calpe, J., Moreno, J., 2007. Sensitivity analysis of the Fraunhofer Line Discrimination method for the measurement of chlorophyll fluorescence using a field spectroradiometer. In: 2007 IEEE International Geoscience and Remote Sensing Symposium. IEEE, pp. 3756–3759.

Atherton, J., Olascoaga, B., Alonso, L., Porcar-Castell, A., 2017. Spatial variation of leaf optical properties in a boreal forest is influenced by species and light environment. Front. Plant Sci. 8, 309.

Bacour, C., Baret, F., Béal, D., Weiss, M., Pavageau, K., 2006. Neural network estimation of LAI, fAPAR, fCover and LAI×Cab, from top of canopy MERIS reflectance data: Principles and validation. Remote Sens. Environ. 105 (4), 313–325.

Baret, F., Clevers, J.G.P.W., Steven, M.D., 1995. The robustness of canopy gap fraction estimates from red and near-infrared reflectances: a comparison of approaches. Remote Sens. Environ. 54 (2), 141–151.

Béland, M., Baldocchi, D.D., 2021. Vertical structure heterogeneity in broadleaf forests: effects on light interception and canopy photosynthesis. Agric. For. Meteorol. 307, 108525.

Berger, K., Atzberger, C., Danner, M., D'Urso, G., Mauser, W., Vuolo, F., Hank, T, 2018. Evaluation of the PROSAIL model capabilities for future hyperspectral model environments: a review study. Remote Sens. 10 (1), 85.

Braghiere, R.K., Quaife, T., Black, E., Ryu, Y., Baldocchi, D., 2020. Influence of sun zenith angle on canopy clumping and the resulting impacts on photosynthesis. Agric. For. Meteorol. 291, 108065.

Braghiere, R.K., Wang, Y., Doughty, R., Sousa, D., Magney, T., Widlowski, J.L., Longo, M., Bloom, A.A., Worden, J., Gentine, P., Frankenberg, C., 2021. Accounting for canopy structure improves hyperspectral radiative transfer and sun-induced chlorophyll fluorescence representations in a new generation Earth System model. Remote Sens. Environ. 261, 112497.

Chang, T.G., Zhao, H., Wang, N., Song, Q.F., Xiao, Y., Qu, M., Zhu, X.G., 2019. A three-dimensional canopy photosynthesis model in rice with a complete description of the canopy architecture, leaf physiology, and mechanical properties. J. Exp. Bot. 70 (9), 2479–2490.

Chen, J.M., Leblanc, S.G., 1997. A four-scale bidirectional reflectance model based on canopy architecture. IEEE Trans. Geosci. Remote Sens. 35 (5), 1316–1337.

Chen, B., Lu, X., Wang, S., Chen, J.M., Liu, Y., Fang, H., Liu, Z., Jiang, F., Arain, M.A., Chen, J., Wang, X., 2021. Evaluation of clumping effects on the estimation of global terrestrial evapotranspiration. Remote Sens 13 (20), 4075.

Chen, J.M., Menges, C.H., Leblanc, S.G., 2005. Global mapping of foliage clumping index using multi-angular satellite data. Remote Sens. Environ. 97 (4), 447–457.

Ciganda, V., Gitelson, A., Schepers, J., 2008. Vertical profile and temporal variation of chlorophyll in maize canopy: quantitative "crop vigor" indicator by means of reflectance-based techniques. Agron. J. 100 (5), 1409–1417.

Ciganda, V.S., Gitelson, A.A., Schepers, J., 2012. How deep does a remote sensor sense? Expression of chlorophyll content in a maize canopy. Remote Sens. Environ. 126, 240–247.

Croft, H., Chen, J.M., Zhang, Y., Simic, A., Noland, T.L., Nesbitt, N., Arabian, J., 2015. Evaluating leaf chlorophyll content prediction from multispectral remote sensing data within a physically-based modelling framework. ISPRS J. Photogram. Remote Sens. 102, 85–95.

Croft, H., Chen, J.M., Wang, R., Mo, G., Luo, S., Luo, X., He, L., Gonsamo, A., Arabian, J., Zhang, Y., Simic-Milas, A., Noland, T.L., He, Y., Lomolova, L., Malenovsky, Z., Yi, Q., Beringer, J., Aimiri, R., Hutley, L., Arellano, P., Stahl, C., Bonal, D., 2020a. The global distribution of leaf chlorophyll content. Remote Sens. Environ. 236, 111479.

Croft, H., Arabian, J., Chen, J.M., Shang, J., Liu, J., 2020b. Mapping within-field leaf chlorophyll content in agricultural crops for nitrogen management using Landsat-8 imagery. Precis Agric 21, 856–880.

Di Bella, C.M., Paruelo, J.M., Becerra, J.E., Bacour, C., Baret, F., 2004. Effect of senescent leaves on NDVI-based estimates of f APAR: experimental and modelling evidences. Int. J. Remote Sens. 25 (23), 5415–5427.

Duthoit, S., Demarez, V., Gastellu-Etchegorry, J.P., Martin, E., Roujean, J.L., 2008. Assessing the effects of the clumping phenomenon on BRDF of a maize crop based on 3D numerical scenes using DART model. Agric. For. Meteorol. 148 (8–9), 1341–1352.

Ellsworth, D.S., Reich, P.B., 1993. Canopy structure and vertical patterns of photosynthesis and related leaf traits in a deciduous forest. Oecologia 96, 169–178.

Fang, H., Li, W., Wei, S., Jiang, C., 2014. Seasonal variation of leaf area index (LAI) over paddy rice fields in NE China: intercomparison of destructive sampling, LAI-2200, digital hemispherical photography (DHP), and AccuPAR methods. Agric. For. Meteorol. 198, 126–141.

Fang, H., Baret, F., Plummer, S., Schaepman-Strub, G., 2019. An overview of global leaf area index (LAI): methods, products, validation, and applications. Rev.Geophys. 57 (3), 739–799.

Fang, H., 2021. Canopy clumping index (CI): a review of methods, characteristics, and applications. Agric. For. Meteorol. 303, 108374.

Fournier, C., Andrieu, B., 1998. A 3D architectural and process-based model of maize development. Ann Bot 81 (2), 233–250.

Gara, T.W., Darvishzadeh, R., Skidmore, A.K., Wang, T., Heurich, M., 2019. Accurate modelling of canopy traits from seasonal Sentinel-2 imagery based on the vertical distribution of leaf traits. ISPRS J. Photogram. Remote Sens. 157, 108–123.
Gastellu-Etchegorry, J.P., Demarez, V., Pinel, V., Zagolski, F., 1996. Modeling radiative transfer in heterogeneous 3-D vegetation canopies. Remote Sens. Environ. 58 (2), 131–156.
Gastellu-Etchegorry, J.P., Lauret, N., Yin, T., Landier, L., Kallel, A., Malenovský, Z., Bitar, A.A., Aval, J., Benhmida, S., Qi, J., 2017. DART: recent advances in remote sensing data modeling with atmosphere, polarization, and chlorophyll fluorescence. IEEE J. Sel. Top. Appl. Earth Obs. Remote Sens. 10 (6), 2640–2649.
Govind, A., Guyon, D., Roujean, J.L., Yauschew-Raguenes, N., Kumari, J., Pisek, J., Wigneron, J.P., 2013. Effects of canopy architectural parameterizations on the modeling of radiative transfer mechanism. Ecol. Modell. 251, 114–126.
Hagemeier, M., Leuschner, C., 2019. Functional crown architecture of five temperate broadleaf tree species: vertical gradients in leaf morphology, leaf angle, and leaf area density. Forests 10 (3), 265.
Hirose, T., Werger, M.J.A., 1987. Maximizing daily canopy photosynthesis with respect to the leaf nitrogen allocation pattern in the canopy. Oecologia 72, 520–526.
Houborg, R., Soegaard, H., Boegh, E., 2007. Combining vegetation index and model inversion methods for the extraction of key vegetation biophysical parameters using Terra and Aqua MODIS reflectance data. Remote Sens. Environ. 106 (1), 39–58.
Houborg, R., McCabe, M., Cescatti, A., Gao, F., Schull, M., Gitelson, A., 2015. Joint leaf chlorophyll content and leaf area index retrieval from Landsat data using a regularized model inversion system (REGFLEC). Remote Sens. Environ. 159, 203–221.
Hwang, Y., Kim, J., Ryu, Y., 2023. Canopy structural changes explain reductions in canopy-level solar induced chlorophyll fluorescence in Prunus yedoensis seedlings under a drought stress condition. Remote Sens. Environ. 296, 113733.
Jacquemoud, S., Verhoef, W., Baret, F., Bacour, C., Zarco-Tejada, P.J., Asner, G.P., Francois, C., Ustin, S.L., 2009. PROSPECT+ SAIL models: a review of use for vegetation characterization. Remote Sens. Environ. 113, S56–S66.
Jin, S., Sun, X., Wu, F., Su, Y., Li, Y., Song, S., Xu, K., Ma, Q., Baret, F., Jiang, D., Ding, Y., Guo, Q., 2021. Lidar sheds new light on plant phenomics for plant breeding and management: recent advances and future prospects. ISPRS J. Photogramm. Remote Sens. 171, 202–223.
Kimm, H., Guan, K., Jiang, C., Peng, B., Gentry, L.F., Wilkin, S.C., Wang, S., Cai, Y., Bernacchi, C.J., Peng, J., Luo, Y., 2020. Deriving high-spatiotemporal-resolution leaf area index for agroecosystems in the US Corn Belt using Planet Labs CubeSat and STAIR fusion data. Remote Sens. Environ. 239, 111615.
Laurent, V.C., Verhoef, W., Clevers, J.G., Schaepman, M.E., 2011. Inversion of a coupled canopy–atmosphere model using multi-angular top-of-atmosphere radiance data: a forest case study. Remote Sens. Environ. 115 (10), 2603–2612.
Li, F., Hao, D., Zhu, Q., Yuan, K., Braghiere, R.K., He, L., Luo, X., Wei, S., Riley, W.J., Zeng, Y., Chen, M., 2024. Global impacts of vegetation clumping on regulating land surface heat fluxes. Agric. For. Meteorol. 345, 109820.
Li, D., Chen, J.M., Zhang, X., Yan, Y., Zhu, J., Zheng, H., Zhou, K., Yao, X., Tian, Y., Zhu, Y., Cheng, T., Cao, W., 2020a. Improved estimation of leaf chlorophyll content of row crops from canopy reflectance spectra through minimizing canopy structural effects and optimizing off-noon observation time. Remote Sens. Environ. 248, 111985.
Li, J., Zhang, Y., Gu, L., Li, Z., Li, J., Zhang, Q., Zhang, Z., Song, L., 2020b. Seasonal variations in the relationship between sun-induced chlorophyll fluorescence and photosynthetic capacity from the leaf to canopy level in a rice crop. J. Exp. Bot. 71 (22), 7179–7197.
Li, S., Fang, H., Zhang, Y., 2023a. Determination of the Leaf Inclination Angle (LIA) through Field and Remote Sensing Methods: current Status and Future Prospects. Remote Sensing, 15 (4), 946.
Li, H., Zhao, C., Yang, G., Feng, H., 2015. Variations in crop variables within wheat canopies and responses of canopy spectral characteristics and derived vegetation indices to different vertical leaf layers and spikes. Remote Sens. Environ. 169, 358–374.
Lichtenthaler, H.K., Buschmann, C., 2001. Extraction of phtosynthetic tissues: chlorophylls and carotenoids. Curr. Protocols Food Anal. chemistry 1 (1), F2–F4.
Lichtenthaler, H.K., 2007. Biosynthesis, accumulation and emission of carotenoids, α-tocopherol, plastoquinone, and isoprene in leaves under high photosynthetic irradiance. Photosyn. Res. 92, 163–179.
Ma, X., Wang, T., Lu, L., Huang, H., Ding, J., Zhang, F., 2022. Developing a 3D clumping index model to improve optical measurement accuracy of crop leaf area index. Field Crops Res. 275, 108361.
Mõttus, M., 2004. Measurement and modelling of the vertical distribution of sunflecks, penumbra and umbra in willow coppice. Agric. For. Meteorol. 121 (1–2), 79–91.
Malenovský, Z., Regaieg, O., Yin, T., Lauret, N., Guilleux, J., Chavanon, E., Duran, N., Janoutova, R., Delavois, A., Meynier, J., Medjdoub, G., Yang, P., van der Tol, C., Morton, D., Cook, B.D., Gastellu-Etchegorry, J.P., 2021. Discrete anisotropic radiative transfer modelling of solar-induced chlorophyll fluorescence: structural impacts in geometrically explicit vegetation canopies. Remote Sens. Environ. 263, 112564.
Niinemets, Ü., Keenan, T.F., Hallik, L., 2015. A worldwide analysis of within-canopy variations in leaf structural, chemical and physiological traits across plant functional types. New Phytol. 205 (3), 973–993.
Nilson, T., 1971. A theoretical analysis of the frequency of gaps in plant stands. Agric. Meteorol. 8, 25–38.
Pisek, J., Sonnentag, O., Richardson, A.D., Mõttus, M., 2013. Is the spherical leaf inclination angle distribution a valid assumption for temperate and boreal broadleaf tree species? Agric. For. Meteorol. 169, 186–194.
Pisek, J., Adamson, K., 2020. Dataset of leaf inclination angles for 71 different Eucalyptus species. Data Br. 33, 106391.
Ryu, Y., Nilson, T., Kobayashi, H., Sonnentag, O., Law, B.E., Baldocchi, D.D., 2010. On the correct estimation of effective leaf area index: does it reveal information on clumping effects? Agric. For. Meteorol. 150 (3), 463–472.
Van Wittenberghe, S., Alonso, L., Verrelst, J., Moreno, J., Samson, R., 2015. Bidirectional sun-induced chlorophyll fluorescence emission is influenced by leaf structure and light scattering properties—a bottom-up approach. Remote Sens. Environ. 158, 169–179.
Verhoef, W., 1984. Light scattering by leaf layers with application to canopy reflectance modeling: the SAIL model. Remote Sens. Environ. 16 (2), 125–141.
Verrelst, J., Schaepman, M.E., Malenovský, Z., Clevers, J.G., 2010. Effects of woody elements on simulated canopy reflectance: implications for forest chlorophyll content retrieval. Remote Sens. Environ. 114 (3), 647–656.
Verrelst, J., Camps-Valls, G., Muñoz-Marí, J., Rivera, J.P., Veroustraete, F., Clevers, J.G., Moreno, J., 2015. Optical remote sensing and the retrieval of terrestrial vegetation bio-geophysical properties–a review. ISPRS J. Photogramm. Remote Sens. 108, 273–290.
Wang, Y., Kallel, A., Yang, X., Regaieg, O., Lauret, N., Guilleux, J., Chavanon, E., Gastellu-Etchegorry, J.P., 2022. DART-Lux: an unbiased and rapid Monte Carlo radiative transfer method for simulating remote sensing images. Remote Sens. Environ. 274, 112973.
Wang, Q., Li, P., 2013. Canopy vertical heterogeneity plays a critical role in reflectance simulation. Agric. For. Meteorol. 169, 111–121.
Wei, S., Fang, H., Schaaf, C.B., He, L., Chen, J.M., 2019. Global 500 m clumping index product derived from MODIS BRDF data (2001–2017). Remote Sens. Environ. 232, 111296.
Weiss, M., Baret, F., Smith, G.J., Jonckheere, I., 2004. Methods for in situ leaf area index measurement, part II: from gap fraction to leaf area index: retrieval methods and sampling strategies. Agric. For. Meteorol. 121, 17–53.
Xu, M., Liu, R., Chen, J.M., Liu, Y., Shang, R., Ju, W., Wu, C., Huang, W., 2019a. Retrieving leaf chlorophyll content using a matrix-based vegetation index combination approach. Remote Sens. Environ. 224, 60–73.
Xu, M., Liu, R., Chen, J.M., Shang, R., Liu, Y., Qi, L., Croft, H., Ju, W., Zhang, Y., He, Y., Q, F., L, J., Lin, Q., 2022. Retrieving global leaf chlorophyll content from MERIS data using a neural network method. ISPRS J. Photogramm. Remote Sens. 192, 66–82.
Xu, S., Atherton, J., Riikonen, A., Zhang, C., Oivukkamäki, J., MacArthur, A., Honkavaara, E., Hakala, T., Koivumäki, N., Liu, Z., Porcar-Castell, A., 2021. Structural and photosynthetic dynamics mediate the response of SIF to water stress in a potato crop. Remote Sensing of Environment 263, 112555.
Xu, X.Q., Lu, J.S., Zhang, N., Yang, T.C., He, J.Y., Yao, X., Cheng, T., Zhu, Y., Cao, W., Tian, Y.C., 2019b. Inversion of rice canopy chlorophyll content and leaf area index based on coupling of radiative transfer and Bayesian network models. ISPRS J. Photogramm. Remote Sens. 150, 185–196.
Yang, P., Verhoef, W., van der Tol, C., 2017. The mSCOPE model: a simple adaptation to the SCOPE model to describe reflectance, fluorescence and photosynthesis of vertically heterogeneous canopies. Remote Sens. Environ. 201, 1–11.
Yang, X., Li, R., Jablonski, A., Stovall, A., Kim, J., Yi, K., Ma, Y., Baverly, D., Phillips, R., Novick, K., Xu, X., Lerdau, M., 2023. Leaf angle as a leaf and canopy trait: rejuvenating its role in ecology with new technology. Ecol Lett.
Zarco-Tejada, P.J., Miller, J.R., Morales, A., Berjón, A., Agüera, J., 2004. Hyperspectral indices and model simulation for chlorophyll estimation in open-canopy tree crops. Remote Sens. Environ. 90 (4), 463–476.
Zhang, Q., Xiao, X., Braswell, B., Linder, E., Baret, F., Moore III, B., 2005. Estimating light absorption by chlorophyll, leaf and canopy in a deciduous broadleaf forest using MODIS data and a radiative transfer model. Remote Sens. Environ. 99 (3), 357–371.
Zhang, Z., Jin, W., Dou, R., Cai, Z., Wei, H., Wu, T., Yang, S., Tan, M., Li, Z., Wang, C., Yin, G., Xu, B., 2023. Improved estimation of leaf area index by reducing leaf chlorophyll content and saturation effects based on red-edge bands. IEEE Trans. Geosci. Remote Sens.
Zhao, F., Gu, X., Verhoef, W., Wang, Q., Yu, T., Liu, Q., Huang, G., Qin, W., Chen, L., Zhao, H., 2010. A spectral directional reflectance model of row crops. Remote Sens. Environ. 114 (2), 265–285.
Zou, X., Mõttus, M., Tammeorg, P., Torres, C.L., Takala, T., Pisek, J., Mäkelä, P., Stoddard, F.L., Pellikka, P., 2014. Photographic measurement of leaf angles in field crops. Agric. For. Meteorol. 184, 137–146.
Zhao, F., Li, Y., Dai, X., Verhoef, W., Guo, Y., Shang, H., Gu, X., Huang, Y., Yu, T., Huang, J., 2015. Simulated impact of sensor field of view and distance on field measurements of bidirectional reflectance factors for row crops. Remote Sens. Environ. 156, 129–142.
Zou, X., Mõttus, M., 2015. Retrieving crop leaf tilt angle from imaging spectroscopy data. Agric. For. Meteorol. 205, 73–82.